CONFERENCE PRE-PRINT

NONLINEAR SELF-CONSISTENT DYNAMICS OF GEODESIC ACOUSTIC MODES AND ZONAL FLOWS IN TOROIDALLY ROTATING TOKAMAK PLASMAS

V.I. ILGISONIS State Atomic Energy Corporation ROSATOM Moscow, Russian Federation

E.A. SOROKINA
National Research Centre "Kurchatov Institute"
Moscow, Russian Federation
Email: Sorokina_EA@nrcki.com

Abstract

The diagnostics used to study the geodesic acoustic modes (GAMs) in tokamaks allow one to detect the GAM spectra in details, which have no satisfactory explanations within the framework of standard theory. The self-consistent fluid model is developed and successfully applied for the simultaneous simulation of GAMs along with low-frequency zonal flows (ZFs) driven by toroidal plasma rotation in tokamak. The linearized model demonstrates the well-known continuous MHD spectrum of electrostatic axisymmetric oscillations in toroidally rotating tokamak plasmas. The spectrum contains two independent eigenmodes of vastly different frequencies: high-frequency GAM and low-frequency ZF. The nonlinearity results in a much richer spectral pattern exhibiting different oscillations that depend on the equilibrium plasma state, its stability and on the initial level of fluctuations as well. The performed calculations concern both the linearly stable and unstable ZF with the integrals of the motion subject to a control. As a results of calculations, the specific features of the spectra such as GAMs modulation, peak splitting, intermittency and other ones observed within tokamak plasma experiments are presented.

1. INTRODUCTION

Plasma oscillations, which are almost uniform within the magnetic surface, are the essential part of plasma turbulence in tokamaks. They are observed in almost all leading facilities in the form of both geodesic acoustic modes (GAMs) and low-frequency zonal flows (ZFs) [1]. The GAM is a predominantly electrostatic oscillation at frequency of the order of several tens of kHz, while the frequency of ZF is about or less than several kHz only. That is why the conclusive identification of the latter is a challenging task requiring long stationary time sequence data [2].

Early systematic experimental studies of GAMs [3] revealed a number of phenomena, which are not described by the standard theory of a continuous GAM spectrum [4]. In particular, the observations showed that the GAM amplitude tends to be modulated up to 50 % or more, giving the appearance of signal intermittency with a period of a few milliseconds, accompanied by the GAM's spectral peak frequency shifting. Such a behavior could be time-modulation of GAM intensity envelope by a low-frequency ZF. Similar modulation was revealed earlier in numerical simulations of Alfvén drift turbulence [5]. Some manifestations of the modulation effect were observed later on many other tokamaks – see, e.g., Refs. [6]-[10] – and became the subject of intensive research.

In this paper, we present and summarize the results of calculations of the non-linear joint dynamics of GAMs and ZFs in tokamak plasmas showing its relevance to the experimental observations described above. In contrast to [5], the analyzed problem is self-consistent because of exclusive including the interaction of eigenmodes, which can be described by ideal MHD equations. The revealed role of ZFs in the formation of final GAMs spectral pattern appears to be quite important.

With no plasma rotation and no viscosity, the ZF is stationary, i.e., has zero frequency. The finite frequency of ZF arises due to the "unfreezing" of the entropy function from the magnetic surface. The stationary toroidal plasma rotation is considered here as a mechanism for such unfreezing [11], at that the ZF eigenmode can be either oscillatory [12] or linearly unstable [13] depending on the distribution of the equilibrium plasma pressure and density on the magnetic surface.

The simplified model of nonlinear interaction of GAMs and ZFs in toroidally rotating tokamak plasmas was firstly suggested in Ref. [14]. The obtained analytical solution has demonstrated the splitting of the spectral peak of the GAM as a result of its interaction with the ZF of a given amplitude and frequency [15]. In recent paper [16], the nonlinear dynamics of GAM and linearly unstable ZF has been studied self-consistently using the numerical simulations. It was shown there that the nonlinearity results in the stabilization of linearly unstable ZF with a formation of "saturated" low-frequency mode of finite frequency with a consequent generation of multiple GAM side-bands.

Here we consider a more general picture of zonal flow nonlinear dynamics widely varying the initial conditions in the numerical simulations to demonstrate the scope of the process under consideration. We show that in different regimes of nonlinear oscillations a lot of experimentally observed characteristics of GAMs spectral pattern are reproduced that confirms the applicability of the model to describe the real GAMs.

2. MODEL

To describe GAM-ZF nonlinear interaction the conventional electrostatic approximation of the single-fluid ideal MHD equations is used:

$$\rho \left(\frac{\partial \mathbf{v}}{\partial t} + (\mathbf{v} \cdot \nabla) \mathbf{v} \right) = -\nabla p + \frac{1}{c} [\mathbf{j} \times \mathbf{B}], \tag{1}$$

$$\frac{\partial \rho}{\partial t} + \operatorname{div}(\rho \mathbf{v}) = 0, \tag{2}$$

$$\frac{\partial p}{\partial t} + \gamma p \operatorname{div}(\mathbf{v}) + \mathbf{v} \cdot \nabla p = 0, \tag{3}$$

$$\operatorname{div}(\mathbf{j}) = 0,\tag{4}$$

$$[\mathbf{v} \times \mathbf{B}] = c \nabla \Phi. \tag{5}$$

In what follows, the axial symmetry for both the equilibrium plasma state and for the perturbations is assumed to distinguish the considered types of oscillations from the widest spectrum of plasma turbulence. Standard notations for the plasma density ρ , pressure p, velocity \mathbf{v} , current density \mathbf{j} , and magnetic field \mathbf{B} are used; $\gamma = 5/3$ is the specific heat ratio, c is the speed of light, and the CGS units are used. As it follows from Eq. (5), the electric field potential, ϕ , is essentially a function of the magnetic surface.

We apply our model to the equilibrium of toroidally rotating plasma in the tokamak with circular concentric magnetic surfaces. The magnetic field at the surface of radius r is $\mathbf{B} = B_a/R(R_a\mathbf{e}_{\varphi} + r/q\mathbf{e}_{\theta})$. Here B_a is the magnetic field on tokamak magnetic axis, q is the safety factor, R_a is the tokamak major radius, $R = R_a + r \cos\theta$ is the distance from the geometrical center of the torus, φ and θ are the toroidal and poloidal angles, correspondingly. Rotation velocity is $\mathbf{v}_0 = R\Omega(r)\mathbf{e}_{\varphi}$, where Ω is the angular frequency. From here and below the subscript "0" marks stationary quantities.

Toroidal rotation results in a poloidal stratification of plasma pressure and density on the magnetic surface. The poloidal inhomogeneity relates to the velocity of plasma toroidal rotation as follows:

$$p_0 = \bar{p}_0(r) \left(1 + \frac{r}{R_a} \gamma M^2 \cos \theta \right), \quad \rho_0 = \bar{\rho}_0(r) \left(1 + \frac{r}{R_a} \frac{\gamma}{\alpha} M^2 \cos \theta \right).$$

Here \bar{p}_0 , $\bar{\rho}_0$ are the averaged values of equilibrium plasma pressure and density on the magnetic surface, $M = \Omega/\omega_s$ is the toroidal Mach number, $\omega_s = \sqrt{\gamma \bar{p}_0/\bar{\rho}_0}/R_a$, and α is the parameter that describes different types of plasma dynamic equilibrium. Below we consider isothermal ($\alpha = 1$) and isodense ($\alpha \to \infty$) magnetic surfaces. We also used here the known [17] ansatz $p_0 = \rho_0^\alpha \Pi$, where $\Pi = \Pi(r)$ is a surface function, and suppose that the aspect ratio is large, $r/R_a \ll 1$.

Equations (1)-(5) result in the system of coupled PDEs for the perturbed functions, which describe the plasma dynamics taking into account the quadratic nonlinearities in the right-hand sides – see Ref. [14] for the details. In

the dimensionless variables $f(T \equiv t\omega_s, \theta) = \{\tilde{\rho} \equiv (\rho - \rho_0)qR_a/r\bar{\rho}_0, \ \tilde{p} \equiv (p - p_0)qR_a/r\gamma\bar{p}_0, \ \tilde{v} \equiv q(v_{||} - v_{||0})/r\omega_s\}$ and $A(T) \equiv cqd(\phi - \phi_0)/dr/rB_a\omega_s$ the system has the form:

$$\frac{\partial \tilde{\rho}}{\partial T} + \frac{1}{q} \frac{\partial \tilde{v}}{\partial \theta} + A \sin \theta \left(2 + \frac{\gamma}{\alpha} M^2 \right) = \frac{A}{q} \frac{\partial \tilde{\rho}}{\partial \theta}, \tag{6}$$

$$\frac{\partial \tilde{p}}{\partial T} + \frac{1}{q} \frac{\partial \tilde{v}}{\partial \theta} + A \sin \theta (2 + M^2) = \frac{A}{q} \frac{\partial \tilde{p}}{\partial \theta}, \tag{7}$$

$$\frac{\partial \tilde{v}}{\partial T} + \frac{1}{q} \frac{\partial \tilde{p}}{\partial \theta} + 2AM \sin \theta = \frac{A}{q} \frac{\partial \tilde{v}}{\partial \theta},\tag{8}$$

$$\pi \frac{\partial A}{\partial T} - \oint \sin\theta \left(\tilde{p} + M\tilde{v} + \frac{M^2}{2} \tilde{\rho} \right) d\theta = 0.$$
 (9)

The index "||" marks the velocity component along the magnetic field.

Note that quantities $\{\tilde{\rho}, \tilde{p}, \tilde{v}\}$ are poloidally-dependent functions; they will be presented below in the form of $\cos\theta$ and $\sin\theta$ -harmonics (with corresponding subscripts c and s), while A is a magnetic surface function only. Equations (6)-(9) imply all eigenfunctions be strongly localized δ -functions of plasma radius referring to the modes of the continuous spectrum with $\omega = \omega(r)$.

Without the nonlinear terms in the RHSs of Eqs. (6)-(9), the considered system reduces to the well-known MHD dispersion law of zonal flows in toroidally rotating plasmas [17]:

$$\omega^4 - \omega^2 \omega_s^2 \left(2 + \frac{1}{q^2} + 4M^2 + \frac{\gamma M^4}{2\alpha} \right) + \omega_s^4 \frac{\gamma - \alpha}{\alpha} \frac{M^4}{2q^2} = 0.$$
 (10)

The higher root of the dispersion equation (10) gives the GAM frequency, and the lower one – the frequency of ZF. The ZF is aperiodically unstable ($\omega^2 < 0$) at $\alpha > \gamma$ and has a finite frequency in the opposite case. If the stationary toroidal plasma rotation tends to zero, the GAM-branch reduces to the standard expression [4] $\omega_{GAM}^2(M \to 0) = \omega_s^2(2 + 1/q^2)$, while the ZF transforms into the stationary one: $\omega_{ZF}^2(M \to 0) = \omega_s^2 M^4(\gamma - \alpha)/2\alpha(1 + 2q^2) \to 0$.

For the numerical simulation, it is important that Eqs. (6)-(9) possess at least two exact integrals, namely

$$I_1 = A^2 + 0.5(\tilde{v}_s^2 + \tilde{v}_c^2 + \tilde{p}_s^2 + \tilde{p}_c^2) + qM^2(\tilde{p}_c - \tilde{\rho}_c),$$

$$I_2 = 0.5(\tilde{p}_s - \tilde{\rho}_s)^2 + 0.5(\tilde{p}_c - \tilde{\rho}_c)^2 - \frac{qM^2}{\alpha}(\tilde{p}_c - \tilde{\rho}_c)(\gamma - \alpha).$$

The check of their conservation provides a convenient tool for monitoring the numerical calculation procedure, especially in the case of linearly unstable system. All calculations presented below have passed this verification.

3. RESULTS

Due to the nonlinearity, Eqs. (6)-(9) describe a variety of oscillation regimes, the onset of which depends both on the equilibrium parameters (namely, q, M and α) and on the initial conditions. Below we consider two types of equilibria: the stable one with isothermal magnetic surfaces ($\alpha=1$), and the unstable one with isodense magnetic surfaces ($\alpha=1000$), which linear stage is characterized by the exponential growth of ZF amplitude. We also choose q=3. We prescribe the certain initial values of the perturbed electric field for GAM and ZF, $A_{GAM}^0 \equiv A_{GAM}(t=0)$ and $A_{ZF}^0 \equiv A_{ZF}(t=0)$, and calculate the initial values of $\{\tilde{p}, \, \tilde{p}, \, \tilde{v}\}$ using the known linear ratios of these fluctuations to the value of A. Note that |A|=1 means that the angular frequency of the poloidal plasma rotation due perturbed electric field reaches the "longitudinal" sound frequency, ω_s/q .

The presented below examples of the calculated GAM-ZF dynamics obeying Eqs. (6)-(9) are in a correlation with the experiments described in the literature. In the calculations the time interval for spectral analysis is chosen around $600T_s$ ($T_s = 2\pi/\omega_s$) being slightly adjusted to "catch" several total periods of the low-frequency mode. The Cauchy problem for Eqs. (6)-(9) is solved by the Runge-Kutta method of the 4th order, and the amplitude spectra are analyzed using the Fast Fourier Transform (FFT) procedure with a sampling frequency $15\omega_s$.

3.1. Stable equilibrium with iso-thermal magnetic surfaces

In the linearly stable equilibrium both the GAM and the ZF have finite frequency and their amplitudes are mainly determined by the initial conditions. In this case the nonlinear interaction of the modes results in the appearance of GAMs side-bands (satellites) on $\omega_{GAM} \pm \omega_{ZF}$ frequencies. As the amplitude of the ZF increases, the higher side-bands appear. An increase in the toroidal Mach number leads to an up-shift in frequency of ZF, which improves the spectral resolution and makes the fine structure of the spectrum more distinguishable.

3.1.1. GAM side-bands

To demonstrate the appearance of GAM side-bands we choose the regime characterized by the moderate velocity of stationary toroidal plasma rotation with M=0.3, substantial initial amplitude of GAM, $A_{GAM}^0=0.5$, and small amplitude of ZF, $A_{ZF}^0=0.02$. The frequencies of GAM and ZF linear modes calculated from Eq. (10) are $\omega_{GAM}=1.57\omega_S$ and $\omega_{ZF}=0.01\omega_S$.

In Fig. 1a the time evolution of the electric field fluctuations, A(t), is shown. The time signal is a superposition of high-frequency GAM oscillations slightly modulated by the low-frequency ZF. Since $\omega_{GAM} \gg \omega_{ZF}$, there is a lot of GAM oscillations during the period of ZF.

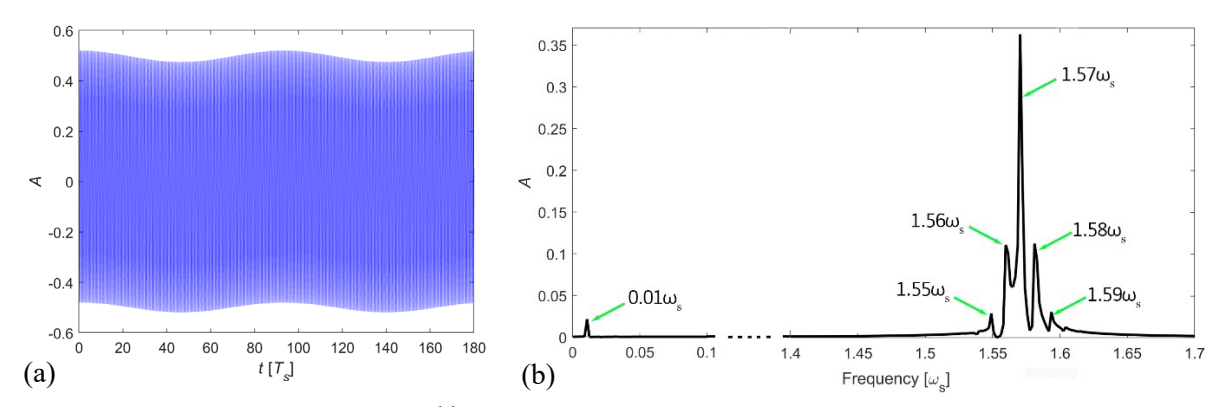


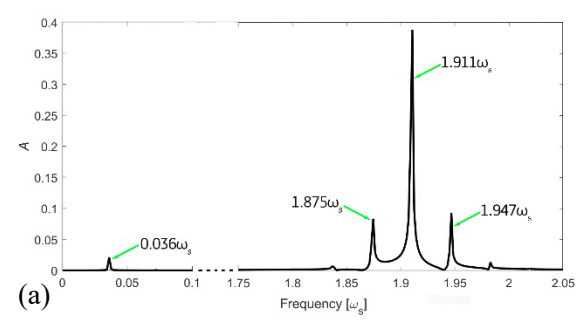
FIG. 1. Time evolution of electric field A(t) (a) and the corresponding spectrum of amplitude (b) in the regime of low modulation. Here M=0.3, $A_{GAM}^0=0.5$, $A_{ZF}^0=0.02$. The length of the FFT analyzed signal is $561T_s$.

The spectral pattern of the above signal is shown in Fig. 1b. Two vastly separated peaks are clearly distinguished: the main peak near the GAM frequency, and the small peak at the near-zero ZF frequency. The high-frequency activity consists of a set of close equidistant peaks divided by the frequency of ZF. The most pronounced peak corresponds to ω_{GAM} and the amplitudes of the side-bands decrease with the distance from it.

An increase in the initial amplitude of the ZF leads to an increase in the number of GAM side-bands and to a change in the structure of the spectrum that we will discuss in the next subsection.

3.1.2. "Two-humped" structure of GAM spectrum

Now let us consider the equilibrium with enhanced velocity of stationary plasma rotation, M=0.6. At higher M, the ZF frequency increases $\sim M^2$ that results in the enhancement of the spectral resolution of the signal. At M=0.6, the frequencies of GAM and ZF are $\omega_{GAM}\approx 1.91\omega_s$ and $\omega_{ZF}\approx 0.036\omega_s$. In Fig. 2 the spectra of amplitudes are shown for the regimes with $A_{GAM}^0=0.5$ and two different values of the ZF initial amplitude: $A_{ZF}^0=0.02$ (Fig. 2a) and $A_{ZF}^0=0.1$ (Fig. 2b).



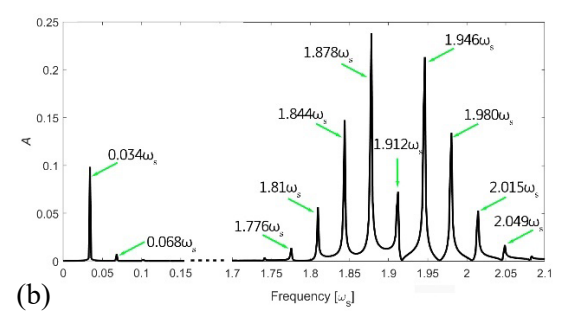


FIG. 2. Spectra of amplitudes of A with different A_{ZF}^0 : $A_{ZF}^0 = 0.02$ (a); $A_{ZF}^0 = 0.1$ (b). Here M = 0.6, $A_{GAM}^0 = 0.5$. The length of the FFT analyzed signal is $582T_s$ for (a) and $615T_s$ for (b).

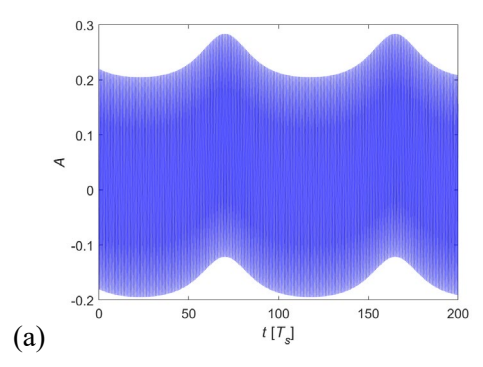
In both cases, the presence of low-frequency ZF results in the appearance of GAM side-bands. Comparing Figs. 2a and 2b, we see that an increase in the initial amplitude of ZF, and, consequently, the rise of nonlinearity, leads (i) to an increase in the amplitude of the GAM side-bands, (ii) to the growth of their number, and (iii) to the formation of a two-humped spectrum structure with a minimum near the original GAM frequency. Such pattern of GAM spectrum, consisting of close equidistant harmonics, was clearly demonstrated in the experiments on tokamak ASDEX Upgrade – cf. Fig. 3b with Fig. 10a in Ref. [3].

3.2. Unstable equilibrium with isodense magnetic surfaces

As we have already mentioned, the equilibrium with isodense magnetic surfaces is linearly unstable with respect to the perturbations of ZF-type, which have zero frequency and finite growth rate $\sim M^2$. In the framework of linear model, it results in the unbounded exponential growth of such perturbations. The nonlinearity results in the saturation of the amplitude of the linearly unstable ZF and its transition into a stable low-frequency mode. The further interaction of this mode with GAMs results in the formation of GAM side-bands and fine structure of spectral pattern.

3.2.1. Interaction of GAM with saturated ZF

Consider the case of linearly unstable system at M=0.3 choosing $A_{GAM}^0=0.2$, $A_{ZF}^0=0.02$. The corresponding time evolution of the electric field fluctuations and their spectrum are shown in Fig. 3. Besides the linear instability, the signal demonstrates strictly periodic oscillations. They contain both the high-frequency component of the GAM and the saturated ZF mode, which appears as a low-frequency modulation of the envelope. Note that the depth of the modulation exceeds the initial value of ZF amplitude that is happen due to its growth during the linear stage of evolution.



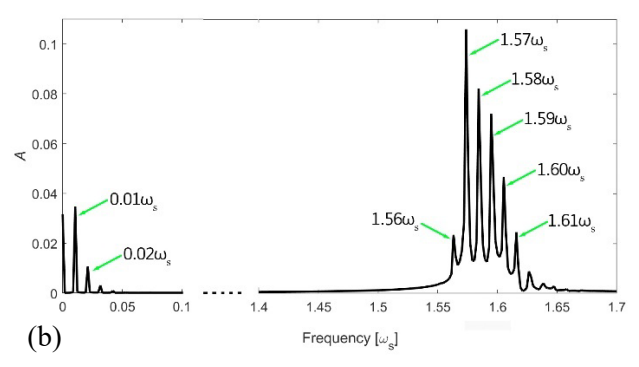


FIG. 3. Time evolution of electric field A(t) (a) and the corresponding spectrum of amplitude (b) in the linearly unstable system. Here M=0.3, $A_{GAM}^0=0.5$, $A_{ZF}^0=0.02$. The length of the FFT analyzed signal is $570T_s$.

In the low-frequency area of the oscillation spectrum, the stabilized ZF activity mainly appears at frequency $0.01\omega_s$; the second harmonic $0.02\omega_s$ and the higher ones are also seen. The GAM spectrum is affected by the low-frequency mode in a manner similar that we discussed in the previous section: the multiply side-bands of GAM separated by the frequency of stabilized ZF are generated, which creates a broadband GAM peak. The complex frequency composition of ZF results in a complex pattern of GAM spectrum as well, in particular, it becomes asymmetric with respect to the original GAM frequency $\omega_{GAM} = 1.57$.

3.2.2. GAM bursts

The linear instability results in the formation of ZF saturated mode even if the initial amplitude of ZF is zero. This is demonstrated by the following calculation at M=0.4, $A_{GAM}^0=0.2$ and $A_{ZF}^0=0.0$. Due to the rather strong stationary rotation, and, as a consequence, the sufficient growth rate of linearly unstable ZF, the amplitude of the saturated ZF mode turns out to be significant and even comparable with the amplitude of the GAM. This is evident from the depth of the envelope modulation in Fig. 4a. The corresponding Fourier spectrum – Fig. 4b – demonstrates complex broadband activity both in the regions of low and high frequencies. The frequency of the main harmonic of saturated ZF is $0.009\omega_S$, at that, the amplitudes of the higher harmonics of the ZF are also significant. The GAM activity is complex: GAM spectrum has the fine structure, which is a set of equidistant side-bands separated exactly by the main harmonic of the saturated ZF. It has an integral two-humped structure, which is a result of interaction with broadband ZF activity. The maximum of the GAM spectrum occurs at the frequency near the linear original GAM frequency $\omega_{GAM}=1.66$, while the spectrum is not centered relative to it.

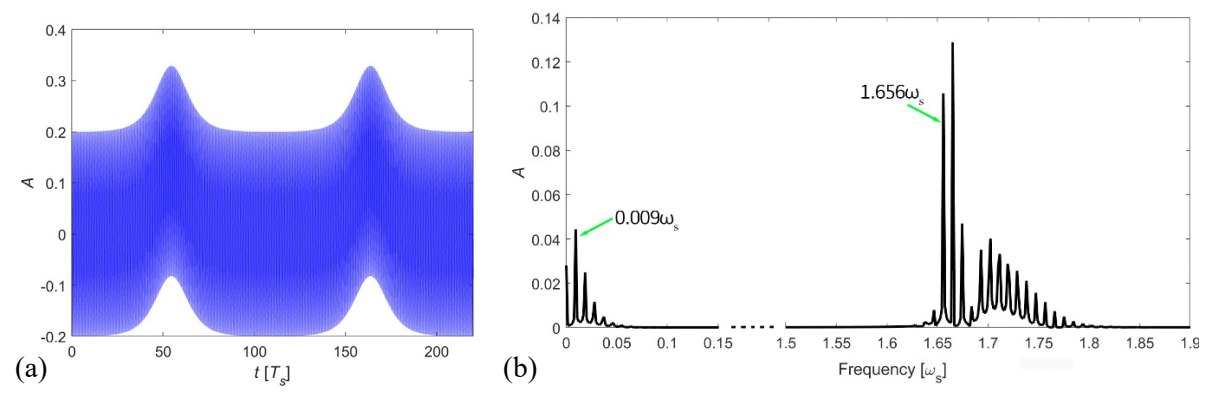


FIG. 4. Time evolution of electric field A(t) (a) and the corresponding spectrum of amplitude (b) in the linearly unstable system with zero initial amplitude of ZF. Here M=0.4, $A_{GAM}^0=0.2$, $A_{ZF}^0=0.0$. The length of the FFT analyzed signal is $645T_c$.

Returning to Fig 4a, note that the signal of the electric field in the considered regime is strictly periodic, but it is sufficiently anharmonic. Moreover, the amplitudes of fluctuations vary strongly in time, so that their modulations are about 50 %. In the spectrogram with a power-cut-off, this is manifested in the appearance of GAM bursts, which occur in correlation with the activity of ZF – see. Fig. 5. Experimental observations of GAM bursts – see, e.g., Refs. [3, 7, 8].

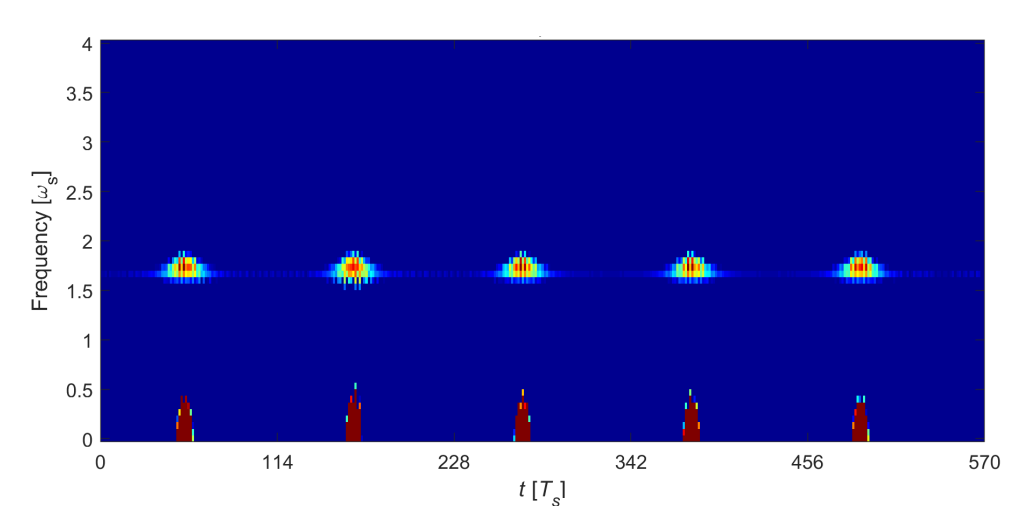


FIG. 5. Spectrogram of plasma electric field fluctuations, A, showing GAM bursts. Here M=0.4, $A_{GAM}^0=0.2$, $A_{ZF}^0=0.0$

4. CONCLUSIONS

The model of nonlinear interaction of GAM and ZF eigenmodes demonstrates typical features of the experimentally observed GAM spectra that shows the relevance of the model to the physics of axisymmetric electrostatic oscillations in tokamak plasmas. It is the influence of the low-frequency ZFs on GAMs that is the mechanism of the periodic modulation and the intermittency of the latter ones. Thus, non-linearity is a significant factor to understand and to interpret the peculiarities of GAM's spectra.

ACKNOWLEDGEMENTS

This work was partly (E.A.) carried out within the state assignment of NRC "Kurchatov Institute".

REFERENCES

- [1] CONWAY, G.D., SMOLYAKOV, A.I., IDO, T., Geodesic acoustic modes in magnetic confinement devices, Nucl. Fusion 62 1 (2022) 013001.
- [2] FUJISAWA, A., A review of zonal flow experiments, Nucl. Fusion 49 1 (2009) 013001.
- [3] CONWAY, G.D., et al, Direct measurement of zonal flows and geodesic acoustic mode oscillations in ASDEX Upgrade using Doppler reflectometry, Plasma Phys. Control. Fusion 47 8 (2005) 1165–1185.
- [4] WINSOR, N., JOHNSON, J.L., DAWSON, J.M., Geodesic acoustic waves in hydromagnetic systems, Phys. Fluids 11 11 (1968) 2448–2450.
- [5] RAMISCH, M., STROTH, U., NIEDNER., S., SCOTT, B., On the detection of Reynolds stress as a driving and damping mechanism of geodesic acoustic modes and zonal flows, New J. Phys. 5 (2003) 12.
- [6] HAMADA, Y., WATARI, T., NISHIZAWA, A., IDO T., KOJIMA, M., KAWASUMI, Y., TOI, K., and the JIPPT-IIU Group, Wavelet and Fourier analysis of zonal flows and density fluctuations in JIPP T-IIU tokamak plasmas, Plasma Phys. Control. Fusion **48** 4 (2006) S177–S191.
- [7] CHENG, J., et al, Density fluctuation of geodesic acoustic mode on the HL-2A tokamak, Nucl. Fusion 49 8 (2009) 085030.
- [8] YASHIN, A.Yu., et al, Geodesic acoustic mode observations in the Globus-M spherical tokamak, Nucl. Fusion **54** 11 (2014) 114015.
- [9] MELNIKOV, A.V., et al, The features of the global GAM in OH and ECRH plasmas in the T-10 tokamak, Nucl. Fusion 55 6 (2015) 063001.
- [10] HILLESHEIM, J.C., PEEBLES, W.A., CARTER, T.A., SCHMITZ L., RHODES, T.L., Experimental investigation of geodesic acoustic mode spatial structure, intermittency, and interaction with turbulence in the DIII-D tokamak, Phys. Plasmas 19 2 (2012) 022301.
- [11] GUAZZOTTO, L., BETTI, R., Magnetohydrodynamics equilibria with toroidal and poloidal flow, Phys. Plasmas 12 5 (2005) 056107.
- [12] WAHLBERG, C., Geodesic acoustic mode induced by toroidal rotation in tokamaks, Phys. Rev. Lett. 101 11 (2008) 115003
- [13] LAKHIN, V.P., ILGISONIS, V.I., SMOLYAKOV, A.I., Geodesic acoustic modes and zonal flows in toroidally rotating tokamak plasmas, Phys. Lett. A **374** 48 (2010) 4872–4875.
- [14] SOROKINA, E.A., Transformation of a geodesic acoustic mode in the presence of a low-frequency zonal flow in a tokamak plasma, JETP Lett. **120** 9–10 (2024) 642–649.
- [15] SOROKINA, E.A., Theoretical model for the experimentally observed GAM's satellites, Proc. 30th IAEA Fusion Energy Conf. (FEC 2025), Chengdu, China, 2025, # 3263.
- [16] SOROKINA, E.A., Nonlinear dynamics of linearly unstable n = 0 electrostatic perturbations in conventional tokamak plasmas, Plasma Phys. Rep. **51** 6 (2025) 665–684.
- [17] HAVERKORT, J.W., DE BLANK, H.J., KOREN, B., The Brunt-Väisälä frequency of rotating tokamak plasmas, J. Comput. Phys. **231** 3 (2012) 981–1001.